How to cite: *Angew. Chem. Int. Ed.* **2025**, *64*, e202424183
doi.org/10.1002/anie.202424183

Halogen–Metal Exchange

Silylation of Aryl and Alkyl Chlorides by a Seven-Membered Dialkoxysilyl Group Si(pan)Me via an In Situ Generated Silylpotassium

Kenshiro Hitoshio, Jun Shimokawa, and Hideki Yorimitsu**

Abstract: Silicon-containing compounds are increasingly vital in pharmaceutical and agrochemical applications, yet existing silylation methods face critical limitations: poor reactivity of unactivated silanes and instability of activated silylation reagents and their products. Here, we present a seven-membered dialkoxysilyl unit, dioxasilepane, abbreviated as Si(pan), that combines exceptional stability with controllable reactivity. We demonstrate a versatile method for Si(pan)Me incorporation into organic molecules through reactions with diverse aryl, alkenyl, and alkyl chlorides. Notably, we have isolated and structurally characterized the key silylpotassium intermediate as its 18-crown-6 complex through X-ray crystallography. Experimental mechanistic studies reveal that this silylpotassium species mediates the transformation primarily through halogen-metal exchange (HME). Computational investigations confirm the HME pathway while suggesting a concurrent S_N2 mechanism for specific primary alkyl chlorides. This methodology establishes Si(pan) as a robust building block for constructing silicon-containing molecular frameworks, addressing a longstanding challenge in organic synthesis.

Introduction

The incorporation of a silicon atom into the molecular skeleton has attracted considerable interest in the fields of pharmaceuticals and agrochemicals. A particularly noteworthy design of the molecule is derived by exchanging a carbon center of the target molecule with a silicon atom, a strategy known as the "silicon switch".[1–6] This exchange causes subtle alterations to the molecular shape, often retaining the fundamentals of biological activity. Moreover, this atom switching modifies the physicochemical properties of the molecule, including lipophilicity, as well as the metabolic pathways. One noteworthy example is the modification of the carbinol moiety of haloperidol, which resulted in the reengineering of the tertiary carbinol moiety into a silanol. This alteration led to a change in the subtype selectivity for a dopamine receptor antagonist (Figure 1a).[7] Additionally, the ketone moiety of the angiotensin converting enzyme (ACE) inhibitor reported by Almquist et al. has been redesigned to a silanediol unit that is bioisosteric to the hydrated form of the ketone.[8–10] These modifications transform known bioactive molecules into new drug-like compounds with distinct physicochemical properties and metabolic pathways. To facilitate the synthesis of these silicon-containing bioactive compounds, there is a strong demand for synthetic methodologies that allow the facile introduction of silicon atoms to the core skeleton of the targeted molecules. Nevertheless, the introduction of silyl groups into complex molecules remains a significant synthetic challenge,[11] as does the evolution of methodologies for constructing these structural units.[12]

We have developed convenient synthetic methods using the dioxasilepanyl group Si(pan) to resolve the dilemma associated with alkoxysilyl groups, where it is challenging to simultaneously achieve enhanced reactivity and stability (Figure 1b).[13–15] To address this issue, we considered the use of stabilization through a cyclic structure. The silyl group exhibits sufficient reactivity due to the presence of two alkoxy groups. The use of steric hindrance alone for stabilization typically results in a reduction in reactivity. In contrast, stabilization by a cyclic structure suppresses excessive molecular flexibility and steric hindrance, thereby highlighting the Lewis acidity of the silicon center. The reactivity of Si(pan)Me has been shown to be both adequate and orthogonal to B(pin) for the Suzuki coupling reaction.[13] The balanced reactivity is primarily due to the kinetic stability as a result of its four flipping methyl groups on the seven-membered cyclic structure that shield the silicon center. Secondly, the cyclic structure also constrains the conformation of the silicate anion intermediate as the alkoxy group assumes both apical and equatorial substitution, forming a 90° coordination angle. This results in thermodynamic stabilization of the dioxasilepane unit by increasing the free energy for silicate formation. Consequently, the chemistry of Si(pan) would

[*] K. Hitoshio, J. Shimokawa, H. Yorimitsu
Department of Chemistry, Graduate School of Science, Kyoto University, Sakyo-ku, Kyoto 606–8502, Japan
E-mail: shimokawa@kuchem.kyoto-u.ac.jp
yori@kuchem.kyoto-u.ac.jp

Additional supporting information can be found online in the Supporting Information section

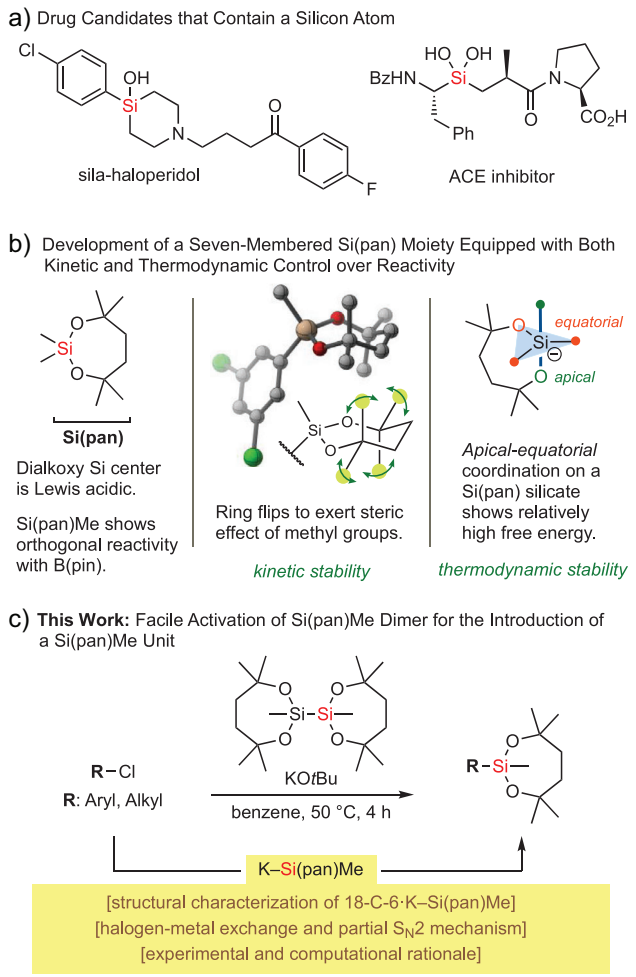

Figure 1. Overview of the current study. 18-C-6 = 18-crown-6 ether.

flourish in organic synthesis by overcoming the problems of unbalanced reactivity and stability that had previously limited the synthetic utility of alkoxysilyl groups.

We focused on the reaction conditions reported by Watanabe on the introduction of the dimethoxymethylsilyl group onto bromobenzene.[16] In their study, putative dimethoxymethylsilylsodium was generated as an intermediate, although no further studies were conducted on the active species and the mechanism. While the dimethoxymethylsilyl group can be activated in the presence of methoxide, the inherent instability of the resulting arylsilane poses a significant challenge to the utilization of this silyl group in organic synthesis. In this context, we postulated the convenient generation of a dioxasilepanyl anion and its use in the silylation reaction based on the contradictory properties of the Si(pan) group, which exhibits both high reactivity and excellent stability (Figure 1c). The research confirmed the structure and reactivity of 18-C-6·K–Si(pan)Me, thereby supporting the intermediate silylpotassium. Further experimental and computational research was conducted to develop the rationale for the plausible reaction mechanism, which involves halogen-metal exchange (HME) and partial S_N2 pathways.

Table 1: Optimization of Silylation Conditions.[a]

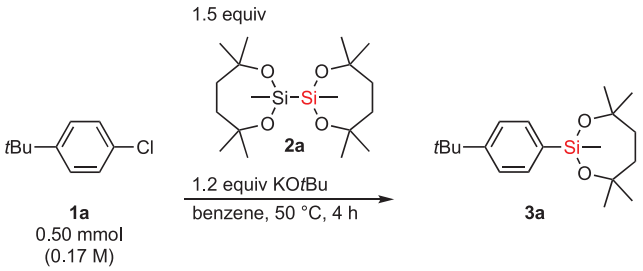

Entry	Deviations from standard conditions	NMR Yield (%) 3a	1a
1	none	98	0
2	*solvent* toluene[b]	94	0
3	hexane	88	0
4	THF	84	0
5	*base* LiO*t*Bu, NaO*t*Bu	0	>95
6	KOMe, $KOSiMe_3$, KHMDS	0	>95
7	CsF, AgF	0	>95
8	rt	90	8
9	4-*t*Bu-C_6H_4Br	82	0
10	4-*t*Bu-C_6H_4I	79	0

[a] More detailed optimization study is described in the Supporting Information; [b] Benzyl–Si(pan)Me (3%) was observed as a byproduct. THF = tetrahydrofuran, KHMDS = potassium hexamethyldisilazide.

Results and Discussion

Optimization and Substrate Scope Survey

As a result of our optimization on the base-mediated silylation of 1-*tert*-butyl-4-chlorobenzene (**1a**) with a newly designed disilane $(Si(pan)Me)_2$ (**2a**), we finally devised the standard conditions for the reaction: **1a** (0.17 M), 1.5 equiv disilane **2a**, 1.2 equiv KO*t*Bu, benzene, 50 °C, 4 h. Table 1 shows the results associated with the differences based on the listed deviations. Under the standard conditions (entry 1), arylsilane **3a** was obtained in 98% nuclear magnetic resonance (NMR) yield. The use of alternative nonpolar solvents, such as toluene and hexane, resulted in a slight decrease in yield (entries 2, 3). The use of toluene as a solvent resulted in the observation of a trace amount (3%) of benzyl–Si(pan)Me. The reaction in THF also provided a satisfactory product yield (entry 4). The use of alternative bases demonstrated even more pronounced differences. In the case of *tert*-butoxide bases (NaO*t*Bu, LiO*t*Bu, entry 5), other bases with a potassium countercation (KOMe, $KOSiMe_3$, KHMDS, entry 6), or fluoride bases such as (CsF, AgF, entry 7), aryl chloride **1a** was almost fully recovered. In these instances, disilane **2a** was predominantly recovered. The reaction proceeded even at room temperature, albeit somewhat slowly (entry 8). Finally, the reaction was observed for aryl bromide and iodide with a slight erosion of the yield (entries 9, 10). Consequently, the conditions in entry 1 were confirmed to be optimal for the current reaction.

To elucidate the characteristics of this reaction, a comparison with other disilanes **2b–2f** was conducted

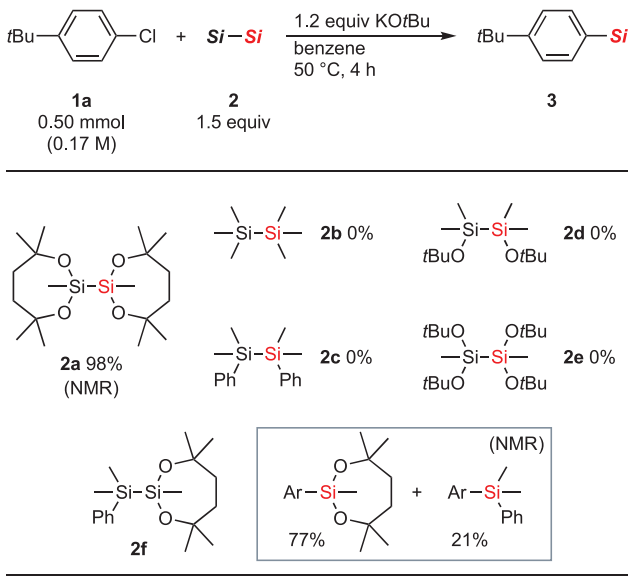

Scheme 1. Scope with Respect to Disilane Reagents.

(Scheme 1). In the case of $(SiMe_3)_2$ (**2b**) and $(SiMe_2Ph)_2$ (**2c**), no consumption of disilanes was observed, which can be attributed to the low Lewis acidity of the silicon centers. Furthermore, the use of dialkoxydisilanes, $(SiMe_2OtBu)_2$ (**2d**) and $(SiMe(OtBu)_2)_2$ (**2e**), did not result in the formation of any silylation products. In these instances, aryl chloride **1a** and disilanes were mostly recovered, with the exception of the volatile **2b**. This result demonstrates the remarkable reactivity of a dioxasilepane moiety, as evidenced by the fact that the sole distinguishing factor between the reactive **2a** and the unreactive **2e** is the seven-membered cyclic structure in **2a**. The distinction between the two lies in the steric hindrance imposed by the conformationally unrestricted *tert*-butoxy substituent. While both compounds exhibit sufficient stability, only **2a**, which features a cyclic structure, allows the *tert*-butoxide ion to approach the silicon center of the disilane. In the case of an unsymmetrical disilane $PhMe_2Si–Si(pan)Me$ (**2f**), the formation of the mixture of the arylsilanes Ar–Si(pan)Me (77%) and Ar–$SiMe_2Ph$ (21%) was observed. This result confirms the importance of using the symmetrical dimer of Si(pan)Me, disilane **2a**.

With the optimized conditions in hand, we next investigated the reaction scope with respect to aryl chlorides (Scheme 2). Isolation of arylsilane **3a** under standard conditions afforded the product in 94% yield. The reaction in hexane was also confirmed to be viable for isolation and gave 85% yield of **3a**. Arylsilanes bearing *p*-, *m*-, and *o*-methyl groups (**3b–3d**) were obtained in excellent yields. 2-Naphthylsilane **3e** and biphenylylsilane **3f** were obtained in 74% and 85% yields, respectively. Arylsilanes bearing an electron rich methoxy group **3g** (87%) or a morpholino group **3h** (93%) at the *para*-positions were obtained in good yields. The transformation of 4-chlorobenzotrifluoride (**1i**) yielded a mixture of *para*-substituted **3i** and *meta*-substituted **3j** in a ratio of 7.1:1, indicating that partial aryne generation was mediated by silylpotassium species via deprotonation followed by the attack of the silyl anion. The pure products **3i** and **3j** were obtained when the corresponding aryl bromides were employed as substrates. The bulky amide group was not compatible with the reaction conditions and **3k** was not observed. The silylated products bearing a benzothiophene **3l** or an indole skeleton **3m** were obtained in moderate yields. The *p*-chloropyridines were silylated in lower yields, irrespective of the 2-methyl or 2-phenyl substituent (**3n**, **3o**). Moreover, the silylation method was applied to bioactive molecules. The desired arylsilane **3p** was obtained in a satisfactory yield using clomipramine (**1p**), which possesses a tertiary amine group. Additionally, a silylated chlorpromazine **3q** bearing a phenothiazine skeleton was successfully synthesized. Alkenyl chlorides could also be silylated, albeit in reduced yields (**3r**, **3s**).

The subsequent investigation focused on the silylation of alkyl halides, as illustrated in Scheme 3. It is noteworthy that the optimized reaction conditions for aryl chlorides are also effective for alkyl chlorides. In particular, the silylation of primary alkyl chlorides was found to be highly efficient. The silylation of *n*-dodecyl chloride (**4a**) led to the formation of the corresponding alkylsilane **5a** in 90% isolated yield. The reaction in hexane confirmed the feasibility of isolation and provided 81% yield of **5a**. In contrast, the use of *n*-dodecyl fluoride was found to be ineffective, whereas the use of the bromide or iodide led to the decomposition of the halide. The reaction exhibited tolerance to a variety of functional groups. The transformation provides branched alkylsilane **5b** (77%), and 1,6-dichlorohexane can be cleanly converted to the corresponding 1,6-disilylated hexane **5c** in 89% yield. The normal benzylic position in the phenyl propane moiety is allowed and **5d** was obtained in 75% yield. Both an internal alkene moiety and an alkyne moiety survived to give the silylated terpene **5e** (42%) and alkyne **5f** (82%). The substrate with a γ-morpholino moiety was compatible and gave **5g** in 80% yield. It is interesting to note that a similar γ-oxy alkyl chloride ($THPO(CH_2)_3Cl$) gave a complex mixture, while the one with an extended methylene unit ($THPO(CH_2)_4Cl$ (**4h**)) gave the silylated product **5h** in 64% yield.[17] A diethyl acetal moiety with a four-carbons tether also survived and **5i** was obtained in 91% yield. Similarly, the phenoxy substrate **4j** and the triisopropylsiloxy one **4k** afforded the corresponding silylated products **5j** and **5k** in 96% and 86% yields, respectively. These results essentially confirmed the functional group compatibility of the current silylation reaction with alkyl chloride substrates. Several substrates showed the formation of unconventional products that illustrate the mechanistic insight of the current reaction. In the case of benzyl chloride (**4l**), the formation of benzylsilane **5l** was observed only in trace amounts, with bibenzyl (**6**) identified as the predominant product. The cyclized product **7** was mainly obtained in 68% yield from 3,3-dimethyl-5-hexenyl chloride (**4m**), in addition to the simple substitution product **5m** (6%). In the case of neophyl chloride (**4n**), only 32% of the silylated product **5n** was obtained, with the concomitant formation of phenylsilane **8** (30%) and isobutylbenzene (**9**). Secondary alkyl chlorides also gave the silylated products, cyclohexyl–Si(pan)Me (**5o**) (44%) and linear secondary silanes **5p** and **5q**, albeit in lower yields. Tertiary alkyl chlorides were found to be incompatible with

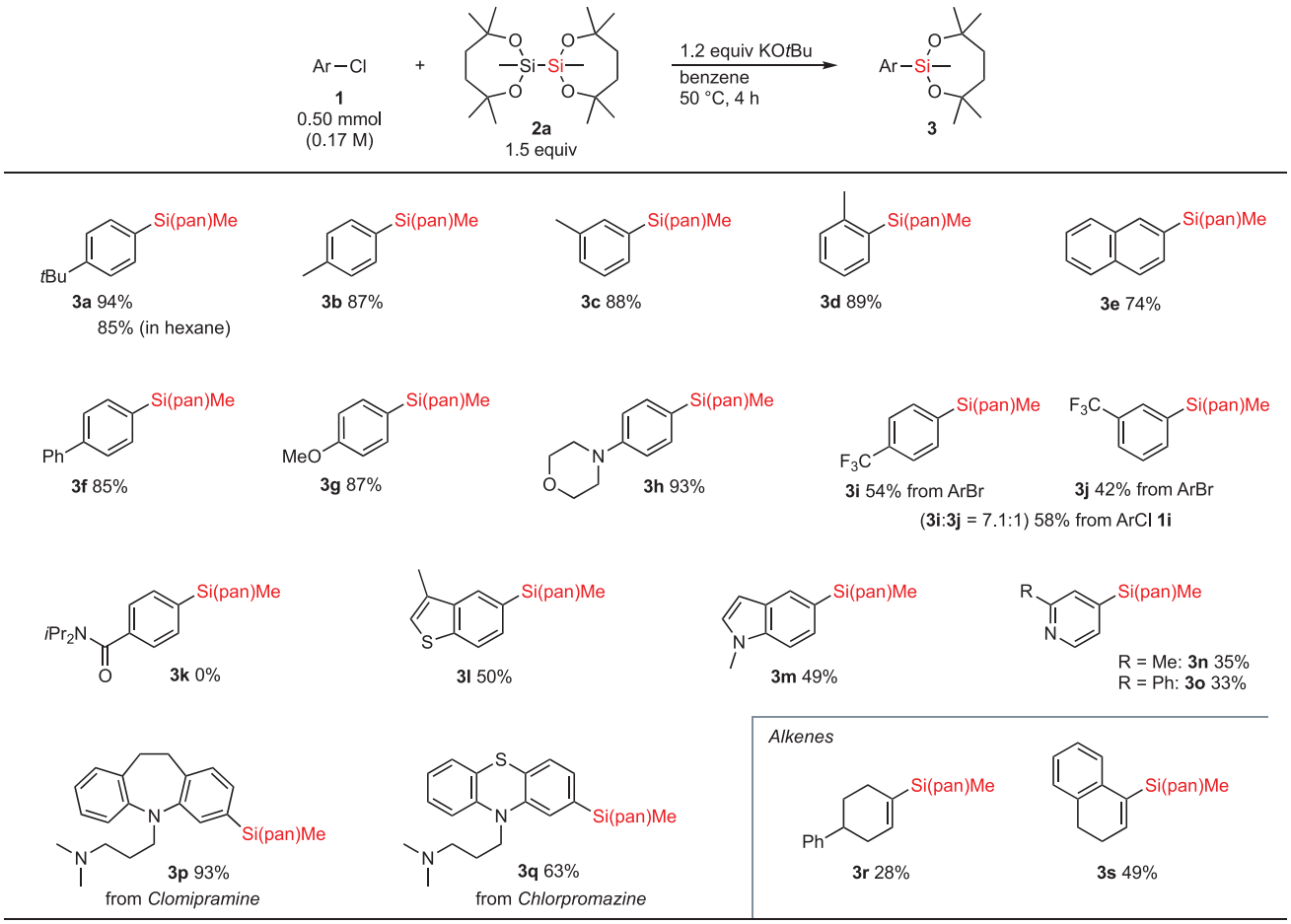

Scheme 2. Substrate Scope with Respect to Aryl Chlorides.[a] a) isolated yields.

this reaction and the silylated **5r** was not observed. The use of the chlorosilane $PhMe_2SiCl$ as an electrophile resulted only in the formation of $PhMe_2SiOtBu$ and no formation of unsymmetrical disilanes was observed.

Confirmation of Silylpotassium Intermediate

Given the expectation that a silylpotassium intermediate should be formed in this reaction, a computational study was conducted to investigate the manner in which the Si–Si bond cleavage occurs through the interaction between $(Si(pan)Me)_2$ (**2a**) and KO*t*Bu (Figure 2a). The structures of both disilane **2a** and KO*t*Bu were modeled in full, with a single η^6-benzene attached to the potassium atom. Our previous study of Si(pan) silicates demonstrated that one of the two alkoxy groups is inclined to occupy an apical position in the silicate, whereas the other occupies an equatorial position.[13] Consequently, it will be intriguing to investigate the silicate structure from which the Si–Si cleavage proceeds. Following the formation of the **INT0** complex, conversion to the silicate **INT1** is achieved via **TS1**, with the *t*BuO unit occupying the apical position. A transition state was next searched for the cleavage of the Si–Si bond, whereas a pathway of the direct cleavage of the Si–Si bond from **INT1** could not be located. However, once **INT1** is transformed to **INT2** via **TS2** by the Berry pseudorotation mechanism, **TS3** for the direct cleavage of the Si–Si bond of the silicate in **INT2** was identified. This transformation ultimately resulted in the formation of **INT3**, which is composed of K–Si(pan)Me and *t*BuO–Si(pan)Me. Despite the absence of a conformer of the silicates with apically oriented silyl groups, such a silicate structure was identified in our calculation along the intrinsic reaction coordinate (IRC) pathway from **INT2** to **TS3**. The silylpotassium species, **SiK1**, is obtained through the almost barrierless removal of *t*BuO–Si(pan)Me. To experimentally confirm the formation of a silylpotassium intermediate, we investigated the formation of single crystals of the silylpotassium species. The reaction of **2a** with KO*t*Bu was conducted in hexane in the presence of 18-crown-6, and the rapid formation of an off-white precipitate was observed. The supernatant was removed under an inert atmosphere, dried, and the crystals were rapidly recrystallized from THF/hexane at −20 °C.[18] From the crystal structure of 18-C-6·K–Si(pan)Me (**10**)[19] (Figure 2b), it can be seen that an ether oxygen atom of the Si(pan) is coordinated to the potassium atom. The bond length around the silicon atom (Si–C = 1.95 Å) is markedly longer than the usual Si–CH_3 distance of 1.86 Å.[20] The distances of the two Si–O bonds are 1.71 Å and 1.74 Å, respectively, which is longer than the typical length of 1.65 Å.

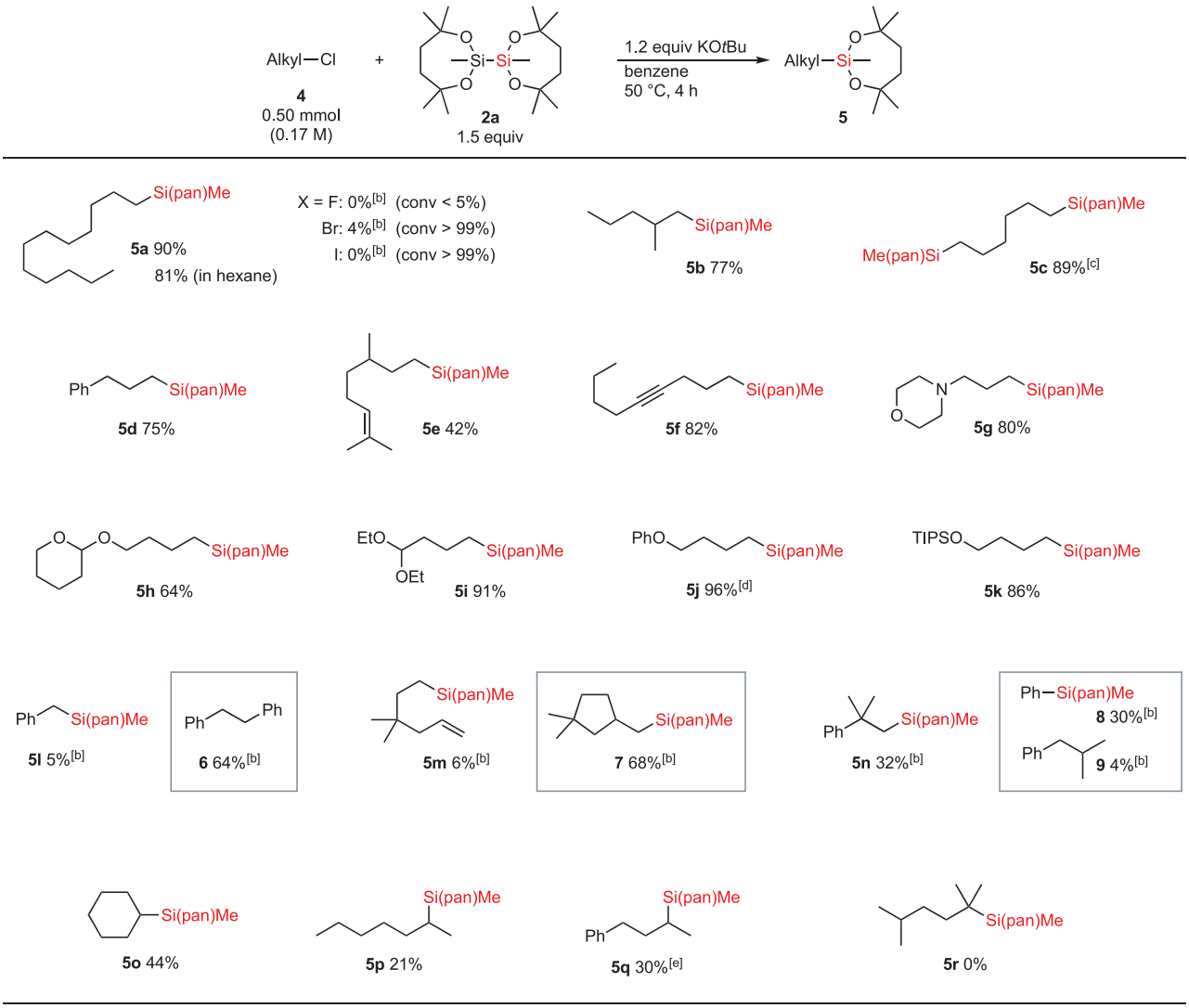

Scheme 3. Substrate Scope with Respect to Alkyl Chlorides.[a] a) Isolated yields. b) NMR yield determined by ^{1}H NMR using mesitylene as an internal standard. c) 3.0 equiv **2a** and 4.0 equiv KO*t*Bu were used. d) 2.0 equiv KO*t*Bu was used. e) Hexane as solvent.

The distance between the silicon and the potassium atoms (3.45 Å) is considerable, and the Wiberg bond index is calculated to be 0.07, indicating that there is minimal actual bonding between Si and K. The bond index between the silicon and the three surrounding atoms is also relatively small (0.51–0.70), albeit within the ordinary level around the silicon atom. The silicon center exhibits a trigonal pyramidal structure, with the bond angles that are smaller than those observed in tetrahedral coordination (109.5°) and are identical in value (103°–105°). Our calculation confirm that the molecular orbitals of the large silyl anion extend outward, and that this silylpotassium **10** exists as a loose ion pair (Figure 2c). This is the inaugural confirmation of the crystal structure of dialkoxysilylpotassium that has been confirmed, while Marshner et al. previously reported the crystal structure of monoalkoxysilylpotassium $(Me_3Si)_2(MeO)SiK{\cdot}18\text{-C-6}$, which exhibits a comparable loose ion pair structure.[21] To confirm the crucial role of the silylpotassium in the current silylation reactions, a reaction between 18-C-6·K–Si(pan)Me (**10**) and *p*-tolyl chloride (**1b**) was attempted (Figure 2d). The reaction afforded the arylsilane **3b**, albeit with diminished efficiency, in a 36% NMR yield with an 86% conversion. Therefore, it is evident that silylpotassium species function as a reaction intermediate in the current silylation reaction.

Mechanism of Silylation of Aryl Chlorides

The reaction mechanism underlying this transformation, in which an aryl halide or alkyl halide reacts with a silyl alkalimetal, remains a topic of ongoing debate within the scientific community. A number of mechanisms have been put forth to explain the conversion (Figure 3a). In the case of aryl halides, HME mechanism and the $S_{RN}1$ reaction type mechanism are typically the subject of discussion. Dervan has confirmed the formation of phenylpotassium in the reaction of iodobenzene with trimethylsilylpotassium, but has reserved judgement on the underlying mechanism, postulating either

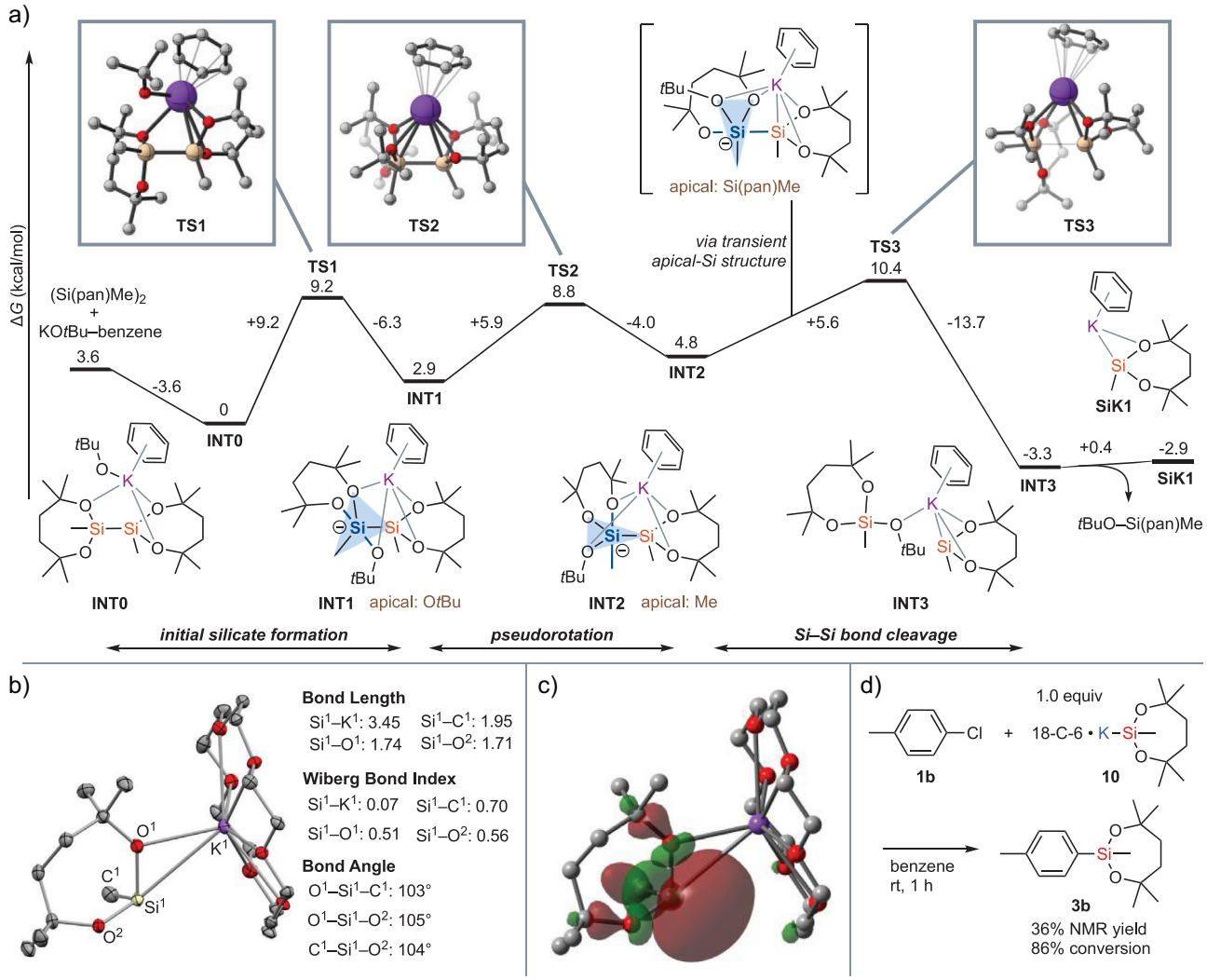

Figure 2. Mechanistic insight for generation of silylpotassium species. a) Energy profile for Si–Si bond cleavage of $(Si(pan)Me)_2$ (**2a**) upon treatment with KO*t*Bu to generate silylpotassium species **SiK1** at the ωB97X-D/def2-TZVPPD in benzene (SMD)//ωB97X-D/def2-SVP level of theory at 323.15 K. b) X-ray crystal structure of 18-C-6·K–Si(pan)Me (**10**) complex. c) Kohn-Sham HOMO of 18-C-6·K–Si(pan)Me (**10**) computed at the ωB97X-D/def2-TZVPPD level of theory using benzene as an implicit solvent; isovalue = 0.03. d) Silylpotassium **10** mediates the silylation reaction of aryl chloride **1b**.

electron transfer or HME.[22] Ito has proposed that the HME is the mechanism to generate an arylpotassium species produced from aryl bromide and silylpotassium,[23–25] and later reported silyllithium similarly behaves to give aryllithium.[26] Strohmann studied a comprehensive investigation into a similar HME mechanism for the generation of aryllithium in the reaction of silyllithium with aryl bromide, while proposing that electron transfer mechanism to play a crucial role for aryl iodides.[27] Additionally, they elucidated the most probable mechanism for the reaction between a silyllithium and an alkyl halide: the S_N2 reaction mechanism is proposed for alkyl chlorides, the HME for alkyl bromides, and electron transfer for alkyl iodides. In contrast, Sakurai put forth the hypothesis that silylsodium undergoes electron transfer to any alkyl halides during the formation of the alkylsodium intermediate.[28–30] Furthermore, Rossi[31–32] and Studer[33] proposed that aryl fluorides react with silyllithiums via S_NAr reaction. Moreover, there are documented instances wherein the S_N2 pathway has been demonstrated to play a pivotal role in the reaction of silyllithium, particularly in the case of alkyl chlorides and bromides.[34–36] These previous reports illustrate the confusion over the reaction mechanism that easily alters upon changing the alkali metals, sp^2/sp^3 hybridization of the carbon, and halogen atoms. Therefore, it is important to determine which of these mechanistic proposals are relevant to our current reaction system.

In order to gain mechanistic insight into the silylation reaction of an organic chloride and a silylpotassium, we conducted experimental and computational mechanistic research. An essential insight into the reaction mechanism of aryl chlorides was gained through the utilization of *N*,*N*-diallyl-2-chloroaniline (**1t**) as the substrate (Figure 3b). The reaction under the standard conditions did not yield a silylated product; rather, only a protonated product **11** with a rearranged allyl group was observed. This distinctive rearrangement of the allyl group is known to proceed by

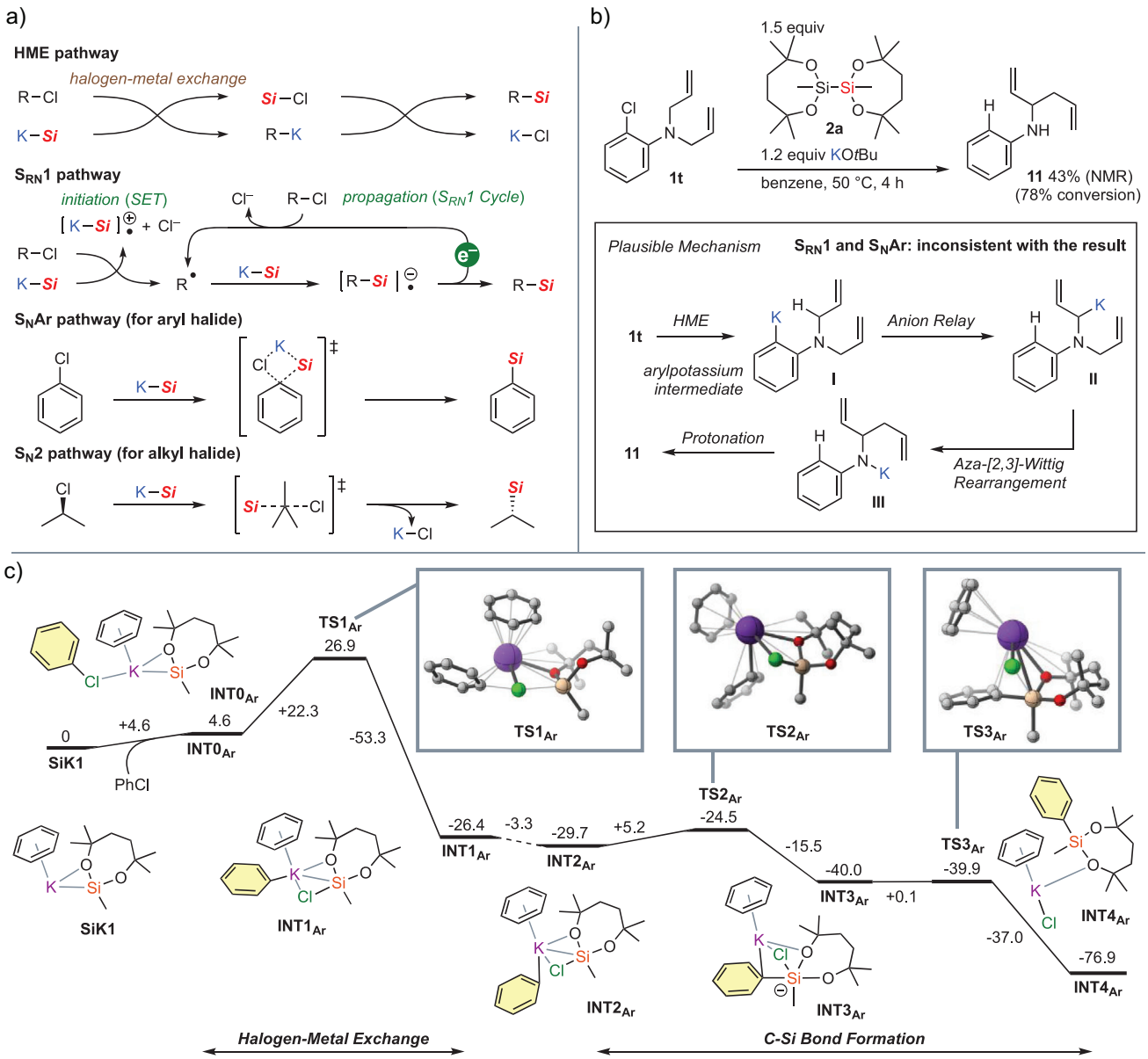

Figure 3. Mechanistic investigation: possible mechanisms for silylation of aryl chlorides. a) Four possible mechanisms for silylpotassium-mediated silylation. b) Silylation of aryl chloride involves arylpotassium intermediate. c) Energy profile for silylation of aryl chloride from the complex **INT0$_{Ar}$** to generate an arylsilane at the ωB97X-D/def2-TZVPPD in benzene (SMD)//ωB97X-D/def2-SVP level of theory at 323.15 K. HME = Halogen-Metal Exchange.

an intramolecular aza-[2,3]-Wittig rearrangement.[37] In the reaction of **1t**, the arylpotassium **I** would be formed by HME followed by an intramolecular proton abstraction, namely intramolecular anion relay,[31] to give the allyllic potassium species **II**. The potassium amide **III** is formed from the allyllic potassium intermediate **II** by an aza-[2,3]-Wittig rearrangement, followed by protonation, to give the product **11**. This is also consistent with the introduction of a hydrogen atom onto the aromatic ring in **11** from the arylpotassium **I**. If the corresponding aryl radical intermediate were involved in the reaction, the radicals would cyclize onto the double bond of the allyl group, thereby forming the 5-membered ring structure of indoline. The absence of such a product in the experiment serves to further exclude the possibility of an aryl radical intermediate. In light of the aforementioned rationale, it is anticipated that aryl chloride will typically react with silylpotassium species, resulting in a potassium–chlorine exchange and the formation of the arylpotassium intermediate. This expectation is consistent with the formation of benzylsilane in Table 1, entry 2, where toluene would be deprotonated by an arylpotassium intermediate and silylated with a chlorosilane generated in situ. The preceding discussion indicates that the $S_{RN}1$ and S_NAr mechanisms are inconsistent with the observed results, thereby supporting the HME mechanism for a reaction involving a silylpotassium and an aryl chloride. It is noteworthy that the HME of aryl chloride by silyl alkali metal has not been previously documented in the literature.

The validity of the reaction mechanism illustrated above was confirmed through a computational study (Figure 3c). The same settings as those utilized in the aforementioned calculations in Figure 2a were employed to model the HME between chlorobenzene and the siliylpotassium species. The silylpotassium **SiK1** is complexed with a chlorobenzene to form $\mathbf{INT0_{Ar}}$, and undergoes the substitution reaction of a silicon species on the chlorine atom proceeds via $\mathbf{TS1_{Ar}}$ with an activation energy of $\Delta G^{\ddagger} = 26.9$ kcal mol^{-1}. This value coincides with the observation that the reaction proceeds under the specified conditions at 50 °C. The arylpotassium species thus generated was confirmed to undergo a transformation from $\mathbf{INT1_{Ar}}$ to $\mathbf{INT2_{Ar}}$. The bond formation between the silicon atom and the anionic carbon atom proceeds through $\mathbf{TS2_{Ar}}$, which constructs a silicate intermediate $\mathbf{INT3_{Ar}}$. This species is then led to the removal of the chloride ion almost barrierlessly through $\mathbf{TS3_{Ar}}$ to form an arylsilane $\mathbf{INT4_{Ar}}$. Therefore, our calculation demonstrated that our experimental result on the HME mechanism for aryl chlorides is reasonable.

Mechanism of Silylation of Alkyl Chlorides

Next we examined the reaction mechanism of the silylation reaction of alkyl chlorides. The propensity for stereo inversion was examined using an optically active secondary alkyl chloride (Figure 4a). The reaction of the optically pure (*S*)-substrate **4q** (99% ee) yielded the alkylsilane **5q** in 29% yield. Oxidative conversion afforded the corresponding secondary alcohol **12**, which was determined by chiral HPLC analysis to be almost racemic (*R*:*S* = 52:48). This result indicates that the reaction for the secondary alkyl chloride does not involve any S_N2 reaction that leads to stereoinversion. Studer et al. also reported a similar decline of stereospecificity for the substitution of a secondary alkyl chloride when silyllithium is used at room temperature.[36] One possible explanation is that an intermediary alkylpotassium or an alkyl radical has racemized during the transformation.

The conversion of **4m** that possesses a terminal alkene illustrates further insights (Figure 4b). The result showed that the predominant silylated product includes a five-membered ring cyclized onto an alkene (**7**, 68%), in addition to the simple silylated product (**5m**, 6%). It is evident that the cyclized product cannot be explained without recourse to an alkylpotassium or an alkyl radical intermediate. This result also indicates that the S_N2 process is not a primary process, even for primary chlorides. This hypothesis is further confirmed by the formation of bibenzyl (**6**) as a byproduct of benzylsilane **5l** from benzyl chloride (**4l**), which suggests that the S_N2 reaction with silylpotassium is more sluggish than the dimerization process.

It is well established that alkali metal silyl anion species function as an electron donors in electron transfer reactions.[28,30] Consequently, it is reasonable to posit that the reaction commences with radical formation initiated by single electron transfer (SET), followed by cyclization and the typical $S_{RN}1$ cycle mechanism.[38,39] Otherwise, alkyl alkali metal species represents a viable intermediate for cyclization to the double bond during the transformation.[40–42] To determine which process is dominant for this transformation, we examined neophyl chloride (**4n**) as the substrate. Under the conditions we developed, silylation product **5n** was obtained in 32% yield in addition to phenylsilane **8** (30%), isobutylbenzene (4%) (Figure 4c). If the reaction proceeds via the $S_{RN}1$ mechanism, which involves the formation of a neophyl radical **IV**, a rapid neophyl rearrangement[43] would occur to form the tertiary radical **V**, thereby providing the products with an isobutylbenzene skeleton. We observed a small amount of isobutylbenzene **9** (4%), which indicates minimal involvement of the radical intermediate. Additionally, if the formation of phenylsilane **8** occurs via the $S_{RN}1$ pathway, it can be postulated that the alkyl radical intermediate must undergo hydrogen atom transfer (HAT) from benzene. However, the higher bond dissociation energy (BDE)[44] of a C–H bond in benzene (113 kcal mol^{-1}) compared to that of alkane (101 kcal mol^{-1} for ethane) precludes the possibility of this HAT process. Thus, the $S_{RN}1$ mechanism is unlikely for the formation of phenylsilane **8**. Conversely, the formation of phenylsilane through intermolecular deprotonation can be explained by the presence of an alkylpotassium intermediate, given the pK_a values of benzene (43) and ethane (50). Therefore, in the case of neophyl chloride (**4n**), alkylpotassium would be formed solely by a halogen-metal exchange mechanism similar to that observed in the case of aryl chloride (Figure 4d). The involvement of the S_N2 reaction in the formation of **5n** can be typically excluded for neophyl chloride. This supposition was further confirmed by the study of the energy profile of these reactions using computational chemistry.

We performed computational verification on the reaction of neophyl chloride (Figure 4e) using the identical setting as that employed for the calculation of the aryl chloride in Figure 3c. Given the experimental results showing low probability of the $S_{RN}1$ reaction via a radical intermediate, we examined which reaction mechanism, HME or S_N2, was the dominant process. The HME pathway transforms $\mathbf{INT0_{HME}}$ to $\mathbf{INT1_{HME}}$ via a substitution reaction on the chlorine atom, occurring through $\mathbf{TS1_{HME}}$. This reaction pathway indicates that an activation energy of 21.2 kcal mol^{-1} is required as $\Delta G^{\ddagger}$, which is sufficiently low for the reaction at 50 °C. Following a change in coordination mode $\mathbf{INT2_{HME}}$, the C–Si bond formation occurs via $\mathbf{TS2_{HME}}$ with a low activation energy of 10.4 kcal mol^{-1}. These findings suggest that the reaction proceeds to $\mathbf{INT3_{HME}}$ through the formation of alkylsilanes. In contrast, the S_N2 reaction pathway to the left of $\mathbf{INT0_{SN2}}$ illustrates that the substitution reaction on the carbon atom necessitates an activation energy of 24.8 kcal mol^{-1} for $\mathbf{TS1_{SN2}}$, which in turn leads to the formation of alkylsilane $\mathbf{INT1_{SN2}}$. Given that the activation energy for $\mathbf{TS1_{HME}}$ is less than that for $\mathbf{TS1_{SN2}}$, it can be concluded that the HME reaction occurs more readily than the S_N2 reaction for neophyl chloride. Experimentally, it is challenging to ascertain whether the reaction of primary alkyl chlorides proceeds either via the HME or S_N2 pathway. From our separately calculated energy diagram for the reaction from chloroethane (Figure S1),[45] it was found that the S_N2 reaction has a lower activation energy than the HME pathway. Therefore, it can be proposed that primary alkyl chlorides, excluding those with a coordinating structure such as an

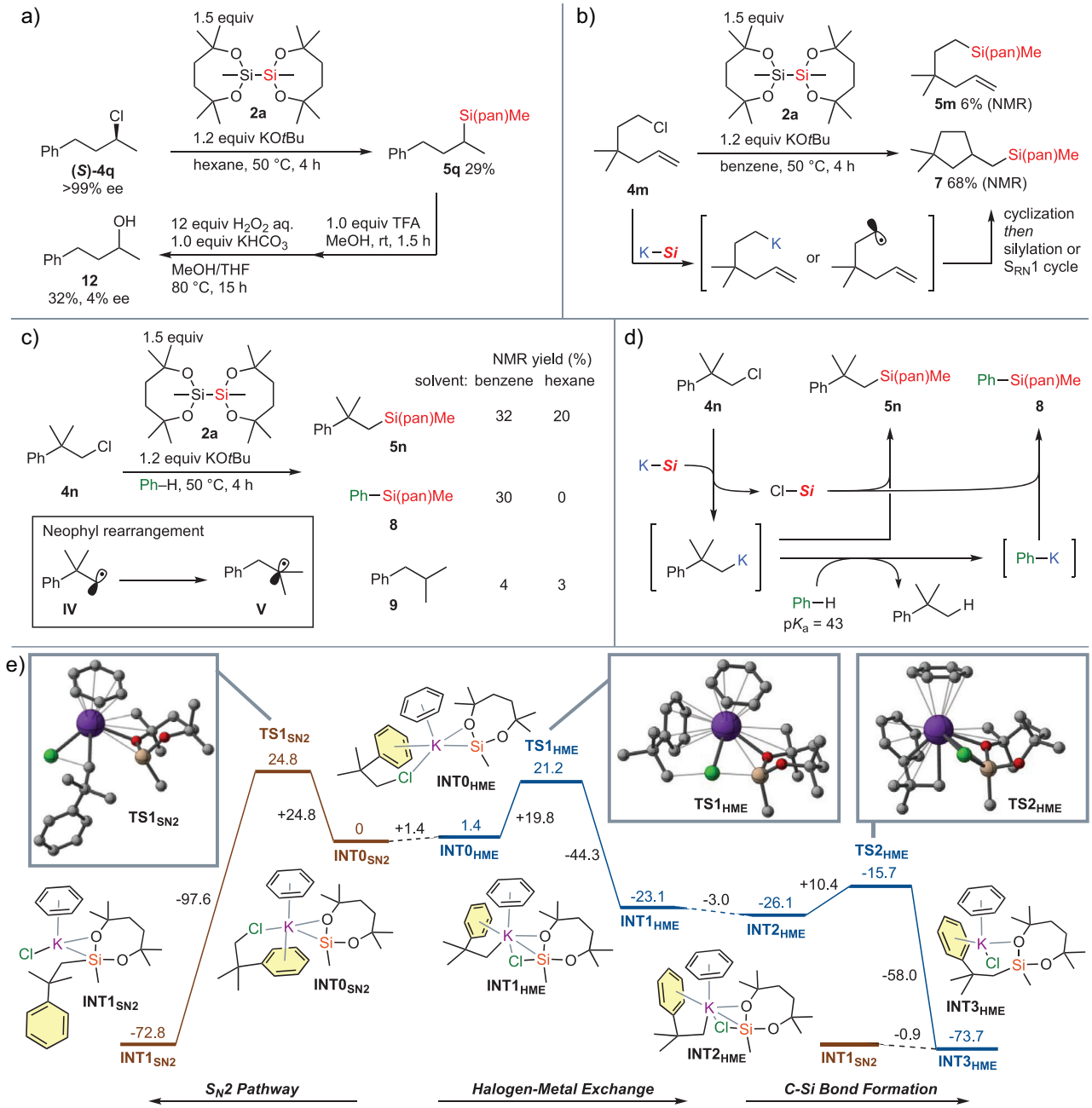

Figure 4. Mechanistic investigation: silylation of alkyl chlorides. a) Silylation of a chiral secondary alkyl chloride indicates negligible S_N2 reaction involvement for a secondary alkyl chloride. b) The formation of a cyclized product suggests an anionic or radical intermediate. c) Anionic intermediate is inferred by the formation of the phenylsilane. d) Plausible anion-mediated mechanism. e) Energy profile for the silylation of neophyl chloride through S_N2 reaction (brown, left) from **INT0$_{SN2}$** and through the sequence of HME reaction from **INT0$_{HME}$** followed by the silylation of neophylpotassium (blue, right) at the ωB97X-D/def2-TZVPPD in benzene (SMD)//ωB97X-D/def2-SVP level of theory at 323.15 K. TFA = trifluoroacetic acid.

alkene in **4m** or a benzene ring in **4n**, may proceed primarily via the S_N2 reaction mechanism.

Conclusion

The present study demonstrates that K–Si(pan)Me, generated in situ from the reactive couple, disilane **2a** and KO*t*Bu, functions as a silylating reagent for structurally diverse aryl, alkenyl, and alkyl chlorides to introduce a synthetically useful Si(pan)Me unit. The structure of the 18-C-6 complex of K–Si(pan)Me was confirmed by X-ray crystallographic analysis, which determined the loose ion-pair structure of a dialkoxysilylpotassium species for the first time. Our mechanistic studies have revealed that the reaction of the silylpotassium species K–Si(pan)Me with aryl chloride proceeds predominantly by a potassium–chlorine exchange reaction, while primary alkyl chlorides may undergo a mixture of varying ratio of

HME reaction and S_N2 reaction in a single reaction. The proposed overall transformation pathway was confirmed to be consistent with our computational studies. We believe that this study not only contributes to the synthesis of functionalized silylated products, but also lays the foundation for the design of new silylation reactions based on our mechanistic insights.

Supporting Information

The authors have cited additional references within the Supporting Information.[46–68]

Acknowledgements

This work was supported by JSPS KAKENHI Grant Numbers JP21H01934, JP19H00895, JST SPRING Grant Number JPMJSP2110 and partly by JST CREST Grant Number JPMJCR19R4, Japan. The authors thank Mr. Yuki Hirata and Prof. Shigeki Matsunaga of Kyoto University for HPLC analysis and Prof. Takashi Kurogi of Kyoto University for X-ray crystallographic analysis.

Conflict of Interests

The authors declare no conflict of interest.

Data Availability Statement

The data that support the findings of this study are available in the supplementary material of this article.

Keywords: Alkoxysilane · Dioxasilepane · Halogen-metal exchange · Silylation · Silylpotassium

[1] R. Tacke, H. Zilch, *Endeavour* **1986**, *10*, 191–197.
[2] P. K. Pooni, G. A. Showell, *Mini-Rev. Med. Chem.* **2006**, *6*, 1169–1177.
[3] N. A. Meanwell, *J. Med. Chem.* **2011**, *54*, 2529–2591.
[4] R. Tacke, S. Dörrich, in *Atypical Elements in Drug Design* (Ed: J. Schwartz), Springer International Publishing, Cham, **2014**, pp. 29–59.
[5] S. Fujii, Y. Hashimoto, *Future Med. Chem.* **2017**, *9*, 485–505.
[6] R. Ramesh, D. S. Reddy, *J. Med. Chem.* **2018**, *61*, 3779–3798.
[7] R. Tacke, F. Popp, B. Müller, B. Theis, C. Burschka, A. Hamacher, M. U. Kassack, D. Schepmann, B. Wünsch, U. Jurva, E. Wellner, *ChemMedChem* **2008**, *3*, 152–164.
[8] R. G. Almquist, J. Crase, C. Jennings-White, R. F. Meyer, M. L. Hoefle, R. D. Smith, A. D. Essenburg, H. R. Kaplan, *J. Med. Chem.* **1982**, *25*, 1292–1299.
[9] S. M. Sieburth, T. Nittoli, A. M. Mutahi, L. Guo, *Angew. Chem., Int. Ed.* **1998**, *37*, 812–814.
[10] M. w. Mutahi, T. Nittoli, L. Guo, S. M. Sieburth, *J. Am. Chem. Soc.* **2002**, *124*, 7363–7375.
[11] J.-L. Panayides, D. L. Riley, F. Hasenmaile, W. A. L. v. Otterlo, *RSC Med. Chem.* **2024**, *15*, 3286–3344.
[12] B. Neil, T. Deis, L. Fensterbank, C. Chauvier, *Angew. Chem. Int. Ed.* **2024**, e202419496.
[13] H. Saito, J. Shimokawa, H. Yorimitsu, *Chem. Sci.* **2021**, *12*, 9546–9555.
[14] K. Hitoshio, H. Maeda, K. Teranishi, J. Shimokawa, H. Yorimitsu, *Chem. Commun.* **2024**, *60*, 7339–7342.
[15] K. Hitoshio, T. Morinaga, R. Sahashi, S. Goshona, H. Yamagishi, H. Saito, J. Shimokawa, H. Yorimitsu, *Synthesis* **2024**, accepted, https://doi.org/10.1055/a-2408-7577.
[16] H. Watanabe, K. Higuchi, M. Kobayashi, M. Hara, Y. Koike, T. Kitahara, Y. Nagai, *J. Chem. Soc. Chem. Commun.* **1977**, 534–535.
[17] Selected unsuccessful substrates are collected in the Supporting Information with a brief classification of the substrates.
[18] See the Supporting Information for the detailed protocol.
[19] These data are provided free of charge by the joint Cambridge Crystallographic Data Centre and Fachinformationszentrum Karlsruhe Access Structures service.
[20] F. H. Allen, O. Kennard, D. G. Watson, L. Brammer, A. G. Orpen, R. Taylor, *J. Chem. Soc. Perkin Trans. 2* **1987**, S1–S19.
[21] P. R. Likhar, M. Zirngast, J. Baumgartner, C. Marschner, *Chem. Commun.* **2004**, 1764–1765.
[22] M. A. Shippey, P. B. Dervan, *J. Org. Chem.* **1977**, *42*, 2654–2655.
[23] R. Uematsu, E. Yamamoto, S. Maeda, H. Ito, T. Taketsugu, *J. Am. Chem. Soc.* **2015**, *137*, 4090–4099.
[24] E. Yamamoto, S. Ukigai, H. Ito, *Chem. Sci.* **2015**, *6*, 2943–2951.
[25] E. Yamamoto, K. Izumi, Y. Horita, S. Ukigai, H. Ito, *Top. Catal.* **2014**, *57*, 940–945.
[26] E. Yamamoto, S. Ukigai, H. Ito, *Synlett* **2017**, *28*, 1250–1257.
[27] C. Däschlein, S. O. Bauer, C. Strohmann, *Eur. J. Inorg. Chem.* **2011**, *2011*, 1454–1465.
[28] H. Sakurai, A. Okada, M. Kira, K. Yonezawa, *Tetrahedron Lett.* **1971**, *12*, 1511–1514.
[29] H. Sakurai, F. Kondo, *J. Organomet. Chem.* **1975**, *92*, C46–C48.
[30] H. Sakurai, A. Okada, H. Umino, M. Kira, *J. Am. Chem. Soc.* **1973**, *95*, 955–956.
[31] A. Postigo, S. E. Vaillard, R. A. Rossi, *J. Organomet. Chem.* **2002**, *656*, 108–115.
[32] A. Postigo, S. E. Vaillard, R. A. Rossi, *J. Phys. Org. Chem.* **2002**, *15*, 889–893.
[33] S. Mallick, P. Xu, E. U. Würthwein, A. Studer, *Angew. Chem. Int. Ed.* **2019**, *58*, 283–287.
[34] F. R. Jensen, D. D. Davis, *J. Am. Chem. Soc.* **1971**, *93*, 4047–4048.
[35] T. Hayashi, Y. Okamoto, M. Kumada, *J. Chem. Soc., Chem. Commun.* **1982**, 1072–1073.
[36] S. Mallick, E.-U. Würthwein, A. Studer, *Org. Lett.* **2020**, *22*, 6568–6572.
[37] M. J. Mealy, M. R. Luderer, W. F. Bailey, M. B. Sommer, *J. Org. Chem.* **2004**, *69*, 6042–6049.
[38] R. A. Rossi, A. B. Pierini, A. B. Peñéñory, *Chem. Rev.* **2003**, *103*, 71–168.
[39] J. I. Bardagí, V. A. Vaillard, R. A. Rossi, in *Encyclopedia of Radicals in Chemistry, Biology and Materials* (Eds: C. Chatgilialoglu, A. Studer), Wiley, Chichester, UK **2012**.
[40] W. F. Bailey, M. J. Mealy, *J. Am. Chem. Soc.* **2000**, *122*, 6787–6788.
[41] W. F. Bailey, J. J. Patricia, V. C. DelGobbo, R. M. Jarret, P. J. Okarma, *J. Org. Chem.* **1985**, *50*, 1999–2000.
[42] M. Yus, R. Ortiz, F. F. Huerta, *Tetrahedron* **2003**, *59*, 8525–8542.
[43] Z.-M. Chen, X.-M. Zhang, Y.-Q. Tu, *Chem. Soc. Rev.* **2015**, *44*, 5220–5245.
[44] S. J. Blanksby, G. B. Ellison, *Acc. Chem. Res.* **2003**, *36*, 255–263.
[45] Details are described in the Supporting Information.
[46] J. Qiu, L. Wang, M. Liu, Q. Shen, J. Tang, *Tetrahedron Lett.* **2011**, *52*, 6489–6491.
[47] N. Schröder, J. Wencel-Delord, F. Glorius, *J. Am. Chem. Soc.* **2012**, *134*, 8298–8301.

[48] G. L. Tolnai, S. Ganss, J. P. Brand, J. R. M. Waser, *Org. Lett.* **2013**, *15*, 112–115.
[49] A. J. Paterson, C. J. Heron, C. L. McMullin, M. F. Mahon, N. J. Press, C. G. Frost, *Org. Biomol. Chem.* **2017**, *15*, 5993–6000.
[50] M. A. Saputra, L. Ngo, R. Kartika, *J. Org. Chem.* **2015**, *80*, 8815–8820.
[51] W. Su, C. Jin, *Org. Lett.* **2007**, *9*, 993–996.
[52] M. Y. Al-Enezi, E. John, Y. A. Ibrahim, N. A. Al-Awadi, *RSC Adv.* **2021**, *11*, 37866–37876.
[53] C. E. Ayala, A. Villalpando, A. L. Nguyen, G. T. McCandless, R. Kartika, *Org. Lett.* **2012**, *14*, 3676–3679.
[54] B. J. Gregori, M. Nowakowski, A. Schoch, S. Pöllath, J. Zweck, M. Bauer, A. J. v. Wangelin, *ChemCatChem* **2020**, *12*, 5359–5363.
[55] M. Kohr, U. Kazmaier, *J. Org. Chem.* **2023**, *88*, 10869–10880.
[56] R. E. Ruscoe, N. J. Fazakerley, H. Huang, S. Flitsch, D. J. Procter, *Chem. - Eur. J.* **2016**, *22*, 116–119.
[57] J.-D. Chai, M. Head-Gordon, *Phys. Chem. Chem. Phys.* **2008**, *10*, 6615–6620.
[58] F. Weigend, R. Ahlrichs, *Phys. Chem. Chem. Phys.* **2005**, *7*, 3297–3305.
[59] S. Maeda, Y. Harabuchi, M. Takagi, K. Saita, K. Suzuki, T. Ichino, Y. Sumiya, K. Sugiyama, Y. Ono, *J. Comput. Chem.* **2018**, *39*, 233–251.
[60] S. Maeda, K. Ohno, K. Morokuma, *Phys. Chem. Chem. Phys.* **2013**, *15*, 3683–3701.
[61] S. Maeda, Y. Harabuchi, Y. Sumiya, M. Takagi, K. Suzuki, M. Hatanaka, Y. Osada, T. Taketsugu, K. Morokuma, K. Ohno, GRRM17, http://iqce.jp/GRRM/index_e.shtml (accessed date 23 Nov., 2024).
[62] Gaussian 16, Revision B.01, M. J. Frisch, G. W. Trucks, H. B. Schlegel, G. E. Scuseria, M. A. Robb, J. R. Cheeseman, G. Scalmani, V. Barone, G. A. Petersson, H. Nakatsuji, X. Li, M. Caricato, A. V. Marenich, J. Bloino, B. G. Janesko, R. Gomperts, B. Mennucci, H. P. Hratchian, J. V. Ortiz, A. F. Izmaylov, J. L. Sonnenberg, D. Williams-Young, F. Ding, F. Lipparini, F. Egidi, J. Goings, B. Peng, A. Petrone, T. Henderson, D. Ranasinghe, et al., Gaussian, Inc., Wallingford CT, **2016**.
[63] D. Rappoport, F. Furche, *J. Chem. Phys.* **2010**, *133*, 134105.
[64] A. V. Marenich, C. J. Cramer, D. G. Truhlar, *J. Phys. Chem. B* **2009**, *113*, 6378–6396.
[65] C. Y. Legault, CYLview20, Université de Sherbrooke, **2020** (http://www.cylview.org).
[66] L. Longwitz, S. Jopp, T. Werner, *J. Org. Chem.* **2019**, *84*, 7863–7870.
[67] G. Xu, S. Leloux, P. Zhang, J. M. Suárez, Y. Zhang, E. Derat, M. Ménand, O. Bistri-Aslanoff, S. Roland, T. Leyssens, O. Riant, M. Sollogoub, *Angew. Chem., Int. Ed.* **2020**, *59*, 7591–7597.
[68] G. M. Sheldrick, *Acta Crystallogr., Sect. A: Found. Crystallogr.* **2015**, *71*, 3–8.

Manuscript received: December 10, 2024
Revised manuscript received: January 21, 2025
Accepted manuscript online: March 13, 2025
Version of record online: March 24, 2025